

Filler Reinforcement in Electron Beam-Cured Hard Paint Films

MAKI ITOH,* TOSHIAKI SHIOTA, and MINORU NISHIHARA,
*Technical Research Laboratories, Sumitomo Metal Industries, Ltd.,
Amagasaki 660, Japan*

Synopsis

Filler effect on the dynamic mechanical properties of electron beam (EB)-cured hard paint films has been studied. Introducing TiO_2 particles resulted in modulus reinforcement. However, degree of reinforcement was lower compared with that for conventional thermosetting polymers. Although the degree of reinforcement for thermosetting polymers was reported to be greater when the filler-polymer interaction was stronger, the storage moduli of the present composites containing TiO_2 with different surface treatments showed no significant difference. Temperature dependence of the relative modulus and reduced damping can be explained by the particle agglomeration theory. The relative modulus showed no increase and the reduced damping showed no decrease by increasing temperature, respectively. This indicates that the present polymer is hard enough to exert large forces on the agglomerates to destroy them. It is also noted that stress relaxation around a particle will not be involved in increasing temperature, as the cross-linking was carried out at room temperature. Lower filler reinforcement compared with thermosetting polymers can be partly attributed to the particle agglomeration theory.

INTRODUCTION

Through the years, radiation curing has become an accepted means for the curing of organic coatings. The advantages of this technology over thermal curing include higher throughput, minimal floor space, reduced or eliminated solvent emissions, energy savings, and curing at ambient temperature. The two principal sources of radiant energy used in industry are the electron beam (EB) and ultraviolet (UV) light.

Although the mechanism of polymerization is similar for both UV and EB, EB curing technique has some advantages over UV curing: EB curing does not require photoinitiators. Energy consumption is much less than that required for UV curing. Pigmented systems can be cured by EB. UV coatings are more inferior in weatherability.

Since their inception, however, the use of radiation curing in surface coatings and related fields has favored UV rather than EB systems. The predominant reasons must be the higher capital investment for the EB equipment, and its greater complexity involving high vacuum, X-ray shieldings, and inert gas supply. EB curing systems, therefore, should be focused on producing coatings with superior properties.

Recently we have developed EB-cured hard paint films.^{1,2} They exhibited extremely high surface hardness, 7H or higher by pencil hardness test, which

*To whom correspondence should be addressed.

cannot be obtained by thermal curing using coil coating process for precoated steel sheets.

Organic paint films essentially consist of two components, polymers and pigments. Pigments are used (1) as colorants, (2) to give hiding power, (3) to modify the mechanical properties, (4) to improve weatherability and corrosion resistance, and (5) to give functional properties such as electric conductivity. It is well known that small solid fillers such as pigments influence the mechanical properties of polymers as composite materials, and a great many theoretical works have been devoted to the prediction of elastic moduli behavior of filled polymers.³⁻¹⁰

However, less attention in the literature has been directed at filler effect on EB-cured hard paint films. The work reported here describes the filler effect on the dynamic mechanical properties of EB-cured hard paint films, using TiO_2 as a filler.

EXPERIMENTAL

Materials

Multifunctional Acrylates. A multifunctional acrylate oligomer, Aronix M-8100 (Toagosei Chemical Ind.), was used as a base resin. Acrylate monomers were commercial products, and were used as received: trimethylolpropane triacrylate (TMPTA, MW 296, E_u 99), pentaerythritol triacrylate (PETA, MW 298, E_u 99), 1,1,1-*tris*(2-acryloyloxypropoxymethyl)propane (MW 471, E_u 157), tripropyleneglycol diacrylate (MW 300, E_u 150), 3-phenoxy-2-hydroxypropyl acrylate (MW 222, E_u 222), and tetraethyleneglycol mono-phenylether acrylate (MW 324, E_u 324), where E_u is unsaturate equivalent (molecular weight per one acrylate group).

Fillers. Two pigment-grade titanium dioxides (TiO_2) of different surface treatment (denoted as P-1 and P-2: rutile, Ishihara Sangyo) were used. Characteristics of P-1 and P-2 were as follows: average particle diameters were 0.255 and 0.233 μm , densities were 4.2 and 4.0, TiO_2 content were 93 and 88%, and $\text{Al}_2\text{O}_3/\text{SiO}_2$ ratios as surface treatment were 5/1 and 1/1, respectively.

Surface of P-1 was modified by converting hydroxyl groups into their trimethylsilyl ethers.¹¹ First, 500 ml of hexamethyldisilazane was added 64 g of TiO_2 and 2-3 ml of trimethylchlorosilane. After refluxing the solution under nitrogen for three days, the reagents were removed by distillation. The reacted TiO_2 was washed with petroleum ether three times before drying in a vacuum oven.

Procedures

Formulation of Acrylates and Filler Dispersion. The resin composition used in this study consisted of one acrylate oligomer and one to several acrylate monomers. Pigmented formulations were prepared by dispersing a known amount of TiO_2 at several volume fractions in the resins by means of a sand mill containing glass beads (diameter 2 mm). Sand milling was continued for 10-30 minutes, at which time the biggest aggregates were less than 5 μm , as checked by a Hegman gauge.

Curing Procedure. Each formulation was coated on a flat sheet metal substrate using a wire wound rod. The wet films were cured by an electron beam at room temperature under nitrogen using an area beam-type electron beam accelerator manufactured by Nissin-High Voltage Co. It was operated at 175–200 kV, at a beam current up to 20 mA, and with a line speed up to 30 m/min.

Free films were prepared as follows: Coatings were applied to a degreased mild steel sheet without any pretreatment, and were cured by a dosage of 8 Mrad at maximum line speed, 30 m/min. When the coatings were thicker than 100 μm , they were peeled spontaneously by the excess internal stress to give free films.

Testing Methods. The dynamic mechanical properties of the free films were measured using a viscoelasticity spectrometer, Iwamoto Seisakusho model VES-F-III at 20 Hz. Rectangular films with accurately known dimensions of approximately $40 \times 5 \times 0.15$ mm were used.

Knoop indentation hardness was measured following the procedure given in ASTM D 1474-68 (reapproved 1973) using Akashi model MVK-E hardness tester. Knoop hardness number, KHN, was calculated as grams of load per unit area of projected area of the indentation formed. Present conditions were in a film thickness of 60 ± 5 μm at 6 Mrad, and an applied load of 25 g for 20 s.

The exact method for making pencil hardness test is described elsewhere.¹²

The water absorption of the film to its polymer content was measured using free films of about 200 mg in weight and 150 μm in thickness. Films were immersed in water for 48 h, though 24 h was sufficient to reach an equilibrium. After weighing, they were dried in an oven at 110°C to constant weight, and were weighed. The water absorption was calculated as

$$\text{Water absorption} = \frac{(W_w - W_D)}{fW_D} \times 100 \quad (1)$$

where W_w is the weight of the soaked film, W_D is the weight of the dried film, and f is the weight fraction of the polymer in a polymer-filler composite.

RESULTS

Preliminary Experiments

Radiation-curable resin formulations generally consist mainly of acrylate oligomers as base resins, diluted with monomers to reduce the viscosity for better processibility. Paint films obtained by such formulations, however, resulted in low hardness which can be easily available by conventional thermal curing methods.

Here we have focused on hard paint films which cannot be obtained by thermal curing methods using a coil-coating process for precoated steel sheets. The pencil hardness test is generally used to evaluate the hardness of paint films under service conditions in the coating industry. The hardest films obtainable by thermal curing method give the pencil hardness of at most 5 H.

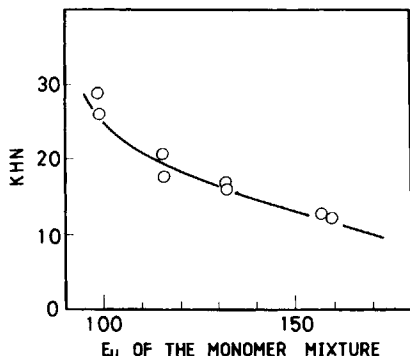


Fig. 1. KHN of electron beam-cured polymers containing 30% of an oligomer as a function of E_u of the monomer mixture.

The content of the oligomer was fixed at 30 wt%, and E_u of the monomer mixture (70 wt%) was varied by changing the mixing ratio of the monomers. In Figures 1 and 2 are plotted KHN and pencil hardness of the paint films cured at 6 Mrad dosage against E_u values of the monomer mixtures, respectively. Both KHN and pencil hardness increased monotonically with a decrease in E_u value, that is, they increased with an increase in cross-link density of the cured polymer. It can be deduced that the resin formulation for a paint film harder than 6 H must contain a large amount of multifunctional acrylate monomers of which E_u values are around 100. This hardness corresponds to the KHN of 25–30, and storage modulus of about 4×10^{11} Pa as shown later. In order to obtain this degree of curing, 6–8 Mrad dosage was sufficient.

In the present study, therefore, resin formulations containing 30% of an oligomer, and 70% of PETA or TMPTA were used as matrix polymers.

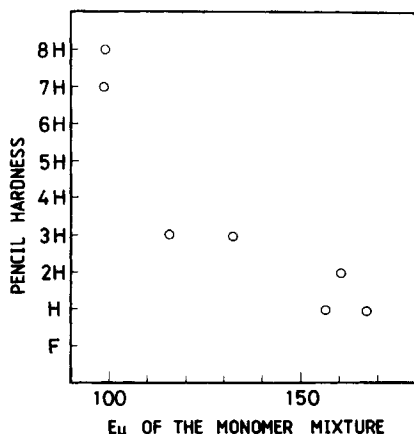


Fig. 2. Pencil hardness of electron beam-cured polymers containing 30% of an oligomer as a function of E_u of the monomer mixture.

Dynamic Mechanical Properties

As with thermosetting resins, generally the storage modulus (E')-temperature curves show drastic decreases in E' by two or three powers of ten in the glass transition region. At glass transition temperature, $\tan \delta$ indicates a sharp peak. These behaviors are reported in literature for thermosetting coatings; glass transition temperatures of 70–130°C for acrylic resins cross-linked with melamines,^{13,14} 60°C for alkyd resins,¹⁵ 20–80°C for unsaturated polyesters,¹⁶ and so on. These polymers showed peak $\tan \delta$ values of about 0.7.

The dynamic mechanical properties as a function of temperature of PETA-based film cured at 8 Mrad dose is shown in Figure 3. The storage modulus showed no drastic decrease up to 200°C and the loss tangent exhibits no sharp peaks. The maximum value of $\tan \delta$ was only 0.07. TMPTA-based polymer films and particle filled films of both PETA- and TMPTA-based formulations showed the same pattern of viscoelastic behavior as in Figure 3.

Effect of Particle Filling on the Storage Modulus

Generally, introducing an inorganic filler into a polymeric material raises the modulus in the glassy region. The viscoelastic properties of TiO_2 filled acrylic resins,¹³ emulsion paint films,¹⁷ waterborne acrylic resins,¹⁸ and alkyd

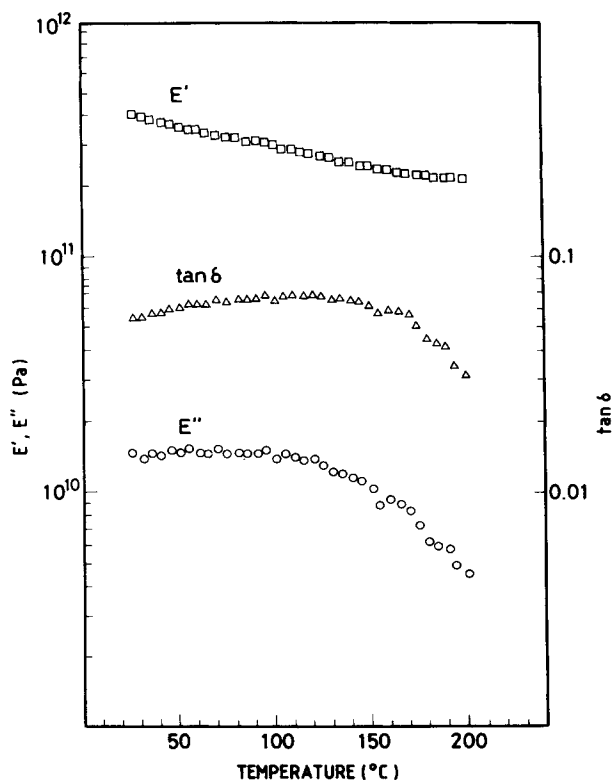


Fig. 3. Dynamic moduli and loss tangent at 20 Hz as a function of temperature for the PETA-based polymer film cured at 8 Mrad.

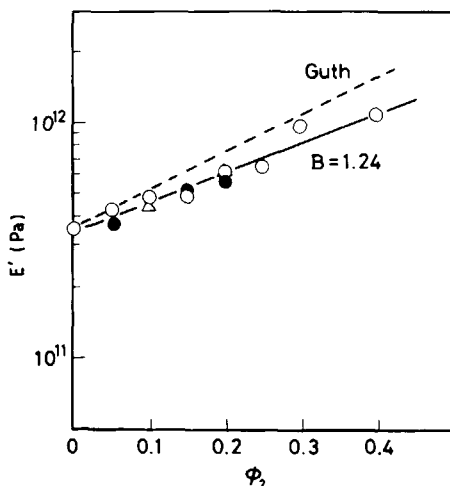


Fig. 4. Dynamic storage moduli as a function of volume loading of filler. PETA-based polymer films with \circ : P-1, \bullet : P-2, and Δ : M-P-1.

resins¹⁵ have been studied previously. Their findings were in accord with modulus reinforcement.

The storage moduli versus volume fraction of P-1 for the PETA based polymer are shown in Figure 4 by closed circle symbols (\circ). ϕ_2 denotes the volume fraction of a filler. Increasing ϕ_2 to 0.4 brings about an increase in the storage modulus. The trend is the same for the TMPTA-based polymer as plotted in Figure 5. The $\log E' - \phi_2$ plot is approximated as following equation:

$$\log E' = \log E'_1 + A\phi_2 \quad (2)$$

where E' denotes the storage modulus of a filled polymer, and E'_1 denotes the

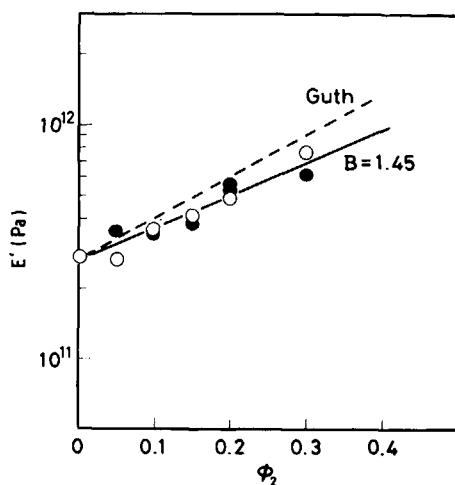


Fig. 5. Dynamic storage moduli as a function of volume loading of filler. TMPTA-based polymer films with \circ : P-1, and \bullet : P-2.

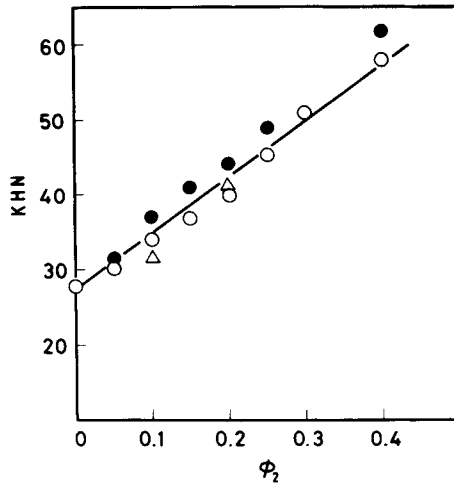


Fig. 6. KHN as a function of volume loading of filler. PETA-based polymer films with \circ : P-1, \bullet : P-2, and Δ : M-P-1.

storage modulus of an unfilled polymer. Values for constant A were 1.23 for the PETA-based polymer and 1.41 for the TMPTA-based polymer, respectively.

In Figures 6 and 7 are shown KHN versus ϕ_2 of P-1 for the PETA and TMPTA-based polymers in closed circle symbols, respectively. In both polymers, KHN increased rectilinearly with an increase in ϕ_2 . The slope was 75 for the PETA-based polymer, and was 85 for the TMPTA-based one. These data show that an indentation hardness of paint films reflects the storage moduli of them.

As a consequence, introduction of TiO_2 into the EB-cured hard paint films brings about an increase in the storage modulus.

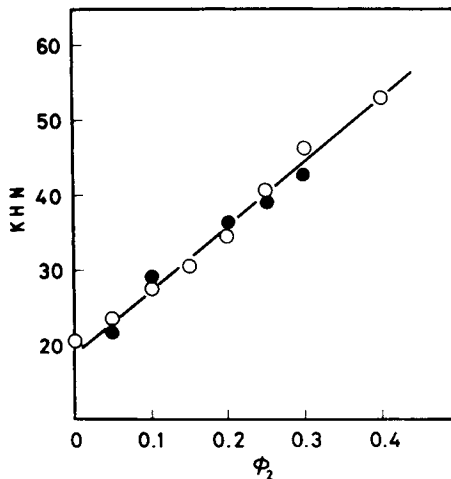


Fig. 7. KHN as a function of volume loading of filler. TMPTA-based polymer films with \circ : P-1, and \bullet : P-2.

Effect of Filler Surface Treatment on Storage Modulus

The surfaces of the TiO_2 used in the present study are treated by Al_2O_3 and SiO_2 . The above mentioned P-1 with the Al_2O_3 to SiO_2 ratio of 5 is widely used in practical organic coatings. It is of interest to study how other grades of TiO_2 with different surface treatments give results. P-2 with the Al_2O_3 to SiO_2 ratio of 1 and modified P-1 by forming trimethylsilyl ether (M-P-1) were used for this purpose. P-2 is expected to have poorer interaction with the polymer than P-1. Infrared (IR) spectrum of M-P-1 showed a decrease in the intensity of OH stretching band at about 3500 cm^{-1} . This indicates that surface OH groups of P-1 is capped by the trimethylsilyl groups. Therefore, M-P-1 will form less hydrogen bonding with matrix polymers than P-1, resulting in poorer adhesion with matrices.

A simple and sensitive method for indication of the interaction between a filler and a polymer by means of water absorption is proposed by Funke.¹⁹ If the water absorption is calculated on the polymer content of the composite film, two different dependencies on ϕ_2 may be encountered in the present case: (1) If the adhesion between the filler and the polymer is strong enough to resist the invading water, the water absorption is independent of ϕ_2 or even decreases with rise of ϕ_2 , (2) a lack of adhesion between the filler and the polymer results in a steady increase in the water absorption with increasing ϕ_2 .

Given in Figure 8 is the water absorption- ϕ_2 plot for the PETA-based polymer with three different TiO_2 . The P-1 filled polymer showed the water absorption independent of ϕ_2 or even decreasing up to 0.3, indicating strong adhesion between the filler and the polymer. The water absorption of the P-2 filled polymer showed a steady increase with increasing ϕ_2 . This shows the lack of adhesion between the filler and the polymer. The M-P-1 filled system showed still greater water absorption, suggesting the poorest adhesion between the filler and the polymer.

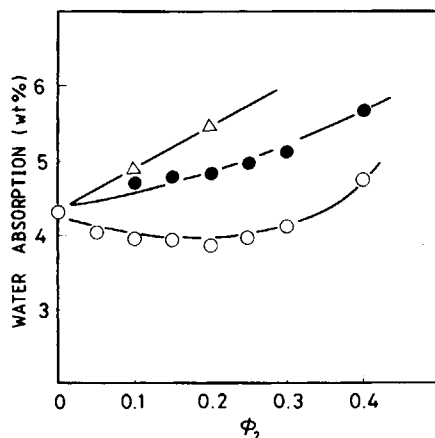


Fig. 8. Water absorption as a function of volume loading of filler. PETA-based polymer films with \circ : P-1, \bullet : P-2, and Δ : M-P-1.

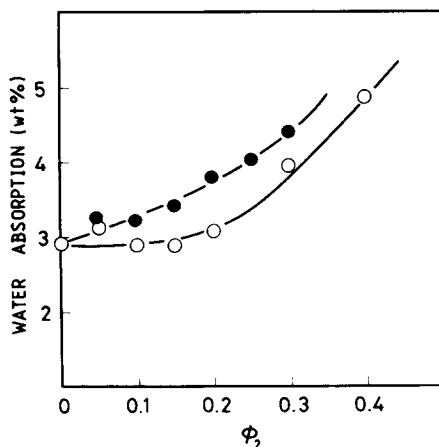


Fig. 9. Water absorption as a function of volume loading of filler. TMPTA-based polymer films with ○: P-1, and ●: P-2.

The water absorption of the TMPTA-based polymer illustrated in Figure 9 shows the same trend. The P-2 filled polymer showed greater water absorption than the P-1 filled polymer. However, even the water absorption of the P-1 filled polymer increased at ϕ_2 larger than 0.2.

The storage moduli of the filled polymers containing TiO_2 with different surface treatments are shown in Figures 4 and 5. Although some differences in the degree of filler reinforcement due to the difference in the filler-polymer interaction was expected, no significant difference in the filler effect was observed among the three TiO_2 filled systems. All $E'-\phi_2$ plots are attributed to equation (2). The three fillers also gave almost the same KHN as shown in Figures 6 and 7.

DISCUSSION

In general, theories of the elastic modulus and other mechanical properties of filled polymers, assuming perfect dispersion of the filler particles, refer to "volume effect" and "surface effect."¹⁰ By volume effect is meant that the introduction of rigid particles in polymers increases the stress at the same strain by reducing the volume of the polymer. This effect is independent of the size and surface characteristics of the filler. The surface effect is an increase in cross-linking by adhesion of the polymer on the filler surface. This effect depends on the degree of interaction between the polymer and the filler particle. According to these theories, stronger adhesion between the polymer and the filler results in higher reinforcement than that is expected by the volume effect.

Pencil hardness, KHN, and 0.5% elastic modulus of alkyd resin paint films containing TiO_2 with different surface treatments was reported by Tsubota et al.¹⁵ TiO_2 with the $\text{Al}_2\text{O}_3/\text{SiO}_2$ ratio of 1/0 or 5/1 (corresponds to P-1) gave harder films than TiO_2 with that of 1/1 (corresponds to P-2). Lee and Nielsen²⁰ studied the surface effect in glass bead-filled butadiene-acrylonitrile

rubbers. The glass beads had one of the following surface treatments: (A) soaked in a dimethyldichlorosilane solution; (B) soaked in a γ -aminopropyl triethyloxysilane and then dried. Treatment A destroys polymer-filler adhesion, and B increases the polymer-filler adhesion. The B-treated beads always gave a higher modulus than the A-treated beads at 60°C, at which temperature the agglomeration of the beads was not so great.

The P-2 and M-P-1 filled polymers in the present study showed greater water absorption than the P-1 filled polymer as provided in Figures 8 and 9. This indicates that the polymer-filler adhesion is greater in P-1-filled systems than in the P-2- or M-P-1-filled systems. Contrary to the expectation, both storage moduli and KHN showed no significant difference among these three fillers. Referring to above-mentioned theories, the volume effect seems to play the major role in the present polymer-filler systems, and the surface effect is less effective.

A simple theoretical equation for the filler reinforcement by volume effect is attributed to Smallwood³ and Guth.⁴ Their equation for the increase in modulus due to a rigid spherical filler is:

$$E = E_1(1 + 2.5\phi_2 + 14.1\phi_2^2) \quad (3)$$

where E is the modulus of the composite, and E_1 is that of matrix polymer. Previously reported TiO_2 filler for melamine-cured alkyd resin films,^{21,22} alkyd enamel films,¹⁵ and polyvinyl acetate or acrylic copolymer emulsion paint films¹⁷ gave greater reinforcement than what was expected by the Guth's equation. This implies that some surface effect is involved in these systems. The Guth plots are indicated by dashed lines in Figures 4 and 5. The filler reinforcement in the present polymer is smaller than the Guth prediction. Consequently, the degree of reinforcement in the present polymer is smaller than in the thermosetting resins.

The Guth equation was originally developed to explain on rubber matrices. Nielsen⁹ has reviewed some theories to deal with rigid matrices: One of the most elaborate and versatile equations for spherical filler particles is due to Kerner:⁵

$$E = E_1 \left\{ \frac{\frac{\phi_2 G_2}{(7 - 5\nu_1)G_1 + (8 - 10\nu_1)G_2} + \frac{\phi_1}{15(1 - \nu_1)}}{\frac{\phi_2 G_1}{(7 - 5\nu_1)G_1 + (8 - 10\nu_1)G_2} + \frac{\phi_1}{15(1 - \nu_1)}} \right\} \quad (4)$$

where E_2 is the modulus of the filler, G_1 is the shear modulus of the polymer, G_2 is the shear modulus of the filler, ϕ_1 is the volume fraction of the polymer, and ν_1 is the Poisson's ratio of the polymer. Nielsen simplified the Kerner's equation as many fillers are much more rigid than matrix polymers:

$$E = E_1 \left[1 + \frac{\phi_2}{\phi_1} \left\{ \frac{15(1 - \nu_1)}{8 - 10\nu_1} \right\} \right] \quad (5)$$

To take polymer-filler interaction into account, Ziegel^{23,24} considered an

immobilization of the matrix polymer at the surface of the dispersed particle. He proposed an effective thickness, r_e , of the interfacial region. If the volume of the particle is enlarged in all dimensions by r_e for spheres, the effective volume fraction of the filler is:

$$\phi_e = \left(1 + \frac{r_e}{r}\right)^3 \phi_2 = B\phi_2 \quad (6)$$

where r is the radius of the filler particle. Substituting equation (6) for ϕ_2 in Eq. (5) yields the following equation:

$$E = E_1 \left[1 + \frac{B\phi_2}{1 - B\phi_2} \left\{ \frac{15(1 - \nu_1)}{8 - 10\nu_1} \right\} \right] \quad (7)$$

Assuming the TiO_2 particle to be spherical, Eq. (7) was applied to the present system, and the B values were calculated. The Poisson's ratio, 0.325, of rigid polystyrene was adapted, as the variation of the value from 0.30 to 0.35 gave little difference on the calculated values of B factor. Equation (7) with the B value of 1.24 for the PETA system and of 1.45 for the TMPTA system accurately describes the variation of storage modulus with filler concentration as shown by the solid lines in Figures 4 and 5. Effective thickness of the interfacial region calculated by Eq. (6) was 0.010–0.015 μm .

The polymer-filler interaction is also affected by the structure of the polymer. Although the water absorption of the P-1-filled polymer was almost constant up to ϕ_2 of 0.3 and slightly increased at ϕ_2 of 0.4 for the PETA-based polymer (Fig. 8), it increased even at ϕ_2 of 0.3 for the TMPTA-based polymer (Fig. 9). This suggests that PETA, because of its OH group, exhibits better adhesion with a filler particle than TMPTA. According to the surface effect theory, the PETA-filler composite is expected to give a higher degree of reinforcement. However, higher degree of filler reinforcement was obtained in the TMPTA-based polymer as shown by the constant A in Eq. (2). This again indicates that the surface effect does not play a major role in the present composite systems.

The above mentioned discussion is based on an assumption of perfect dispersion of the filler particles. In actual practice, however, the filler particles are more or less agglomerated. Figure 10 shows a scanning electron micrograph of P-1-filled PETA-based polymer at ϕ_2 of 0.20. It can be seen that the pigment particles are not perfectly dispersed. TiO_2 with primary diameter of 0.2 μm are agglomerated to give clusters of 0.4 to 1.2 μm in diameter.

Agglomeration of the filler particle increases the elastic modulus by increasing the linear concentration coefficient (k_E)²⁵:

$$E = E_1(1 + k_E\phi_2) \quad (8)$$

In Eq. (8) for the spherical rigid particle dispersion, k_E is 2.50 for dispersed particles, and reaches 4.77 for agglomerates containing cubic-packed spheres.²⁵

Nielsen and Lee^{20,26} have reported the effect of filler particle agglomeration on the dynamic mechanical properties of polymer-filler composites. The tem-

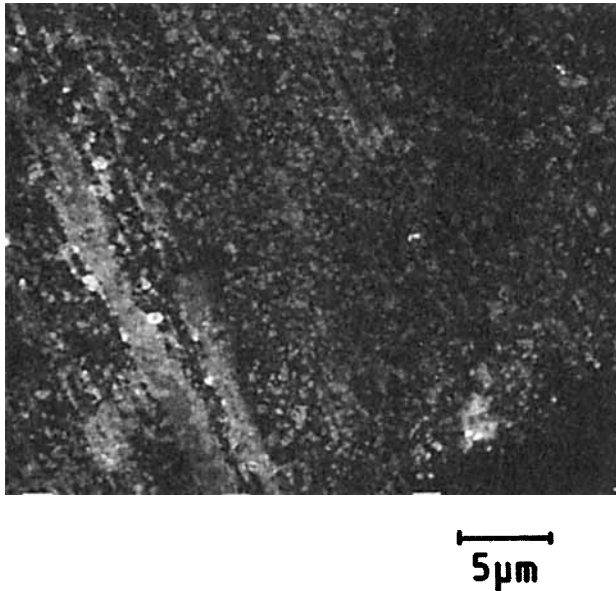


Fig. 10. Scanning electron micrograph of P-1 filled PETA-based polymer. $\phi_2 = 0.20$.

perature dependence of relative modulus and relative or reduced damping were studied to evaluate the effect of the particle-particle contact in agglomerates: Below the glass transition temperature, the relative modulus (E/E_1) increases by increasing temperature. This is because: (1) At low temperature, as the polymer can exert large forces on the agglomerates because of its high modulus, a great deal of particle-particle motion should take place, namely, the agglomerates are broken. Thus, the relative modulus decreases. On increasing the temperature, the polymer softens, exerting less force on the agglomerated particles, so that there is a smaller probability of particle-particle motion. This increases the relative modulus. (2) For a thermosetting resin matrix, stress develops around a particle as the composite cools after curing, according to the difference in thermal expansion coefficients. Since polymers have nonlinear stress-strain curves, the elastic modulus decreases with stress. With increasing temperature, the stress relaxes to give higher relative modulus.²⁷

Figure 11 plots the temperature dependence of the relative modulus at ϕ_2 of 0.20 for the present polymers. As the polymers are supposed to be in the glasslike region, the above mentioned behavior predicted by Nielsen was expected. However, the relative modulus shows no increase with increasing temperature. This is indicative of two characteristics of the present system. First, the polymer must be hard enough to exert large forces on the agglomerates to destroy them even at high temperature. Second, the stress-relaxation process is not involved in increasing temperature, because the polymerization is carried out at room temperature.

According to Nielsen, relative damping (Δ/Δ_1) decreases with an increase in temperature below a glass transition temperature,^{20,26} where Δ is the damping of the composite, and Δ_1 is that of the unfilled polymer. This behavior also

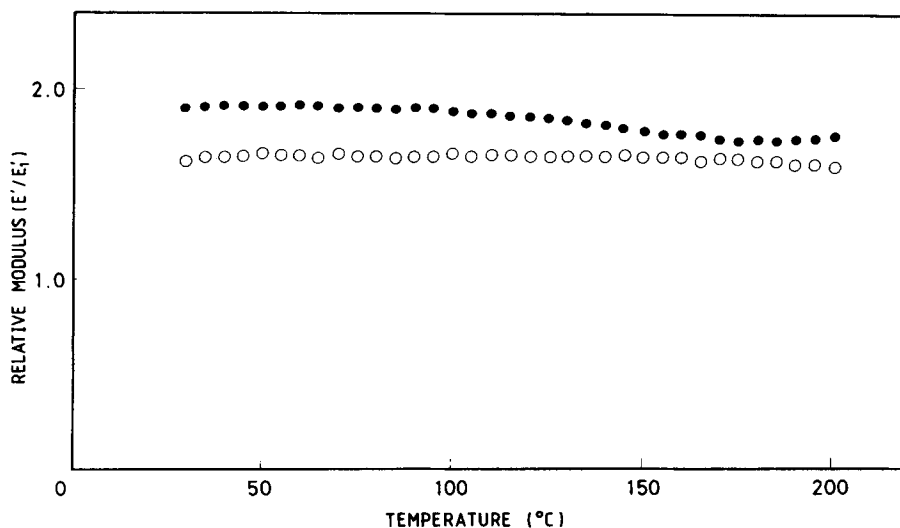


Fig. 11. Relative storage modulus as a function of temperature for ○: PETA-based polymer, and ●: TMPTA-based polymer. $\phi_2 = 0.20$.

can be explained by the mechanism applied for the relative modulus behavior. The additional damping resulting from the presence of the filler particles arises from the frictional heat generated by the slippage between particle and particle, or particle and polymer. Part of the temperature dependence below the glass transition temperature may be due to a decreased particle motion within agglomerates as the polymer softens with rising temperature.

If there are no particle-particle contacts and no slippage at the polymer-particle interfaces, the damping of a composite should be to a first approximation given by

$$\Delta = \Delta_1 \phi_1 \quad (9)$$

Thus the reduced damping, $\Delta/\Delta_1\phi_1$, should be about 1.0 in this case. The reduced damping will be greater than 1.0 if there are additional damping mechanisms provided by the filler such as particle-particle friction. As ϕ_1 is constant, the reduced damping will decrease with increasing temperature.

The reduced damping of the present composite at ϕ_2 of 0.20 is plotted against temperature in Figure 12. Again the behavior was contrary to that observed for conventional thermosetting resins reported by Nielsen.²⁶ The reduced damping showed no decrease with increased temperature. This indicates that the polymer does not soften at high temperature to exert less force on the agglomerates. The reduced damping value was greater than 1.0, indicating that additional damping rising from particle-particle or particle-polymer friction is involved.

As discussed, by comparing with Guth prediction in Figures 4 and 5, the degree of particle reinforcement in the present polymer is smaller than that in the thermosetting polymers. This can be explained partly by the particle agglomeration theory. The present polymer exerts greater force on the agglomerated filler particles than the ordinary paint film resins, so that the

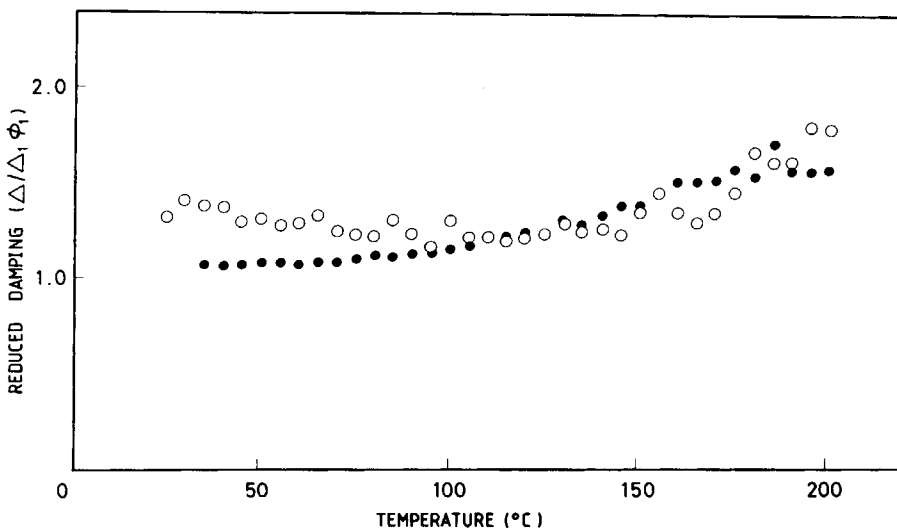


Fig. 12. Reduced damping as a function of temperature for \circ : PETA-based polymer, and \bullet : TMPTA-based polymer. $\phi_2 = 0.20$.

additional reinforcement effect by the particle agglomeration will be reduced in the present composites. Another possible explanation is that greater polymer modulus will reduce the degree of filler reinforcement by reducing the E_2/E_1 ratio. This can be predicted by Eq. (4).

These explanations can be also adapted to interpret the differences in the degree of the particle reinforcement between the PETA and TMPTA systems. The storage modulus of the unfilled polymer is greater in PETA-based polymer than in the TMPTA-based polymer, resulting in greater reinforcement for the TMPTA-based polymer than for the PETA-based polymer as mentioned for Eq. (2).

CONCLUSIONS

Introducing TiO_2 to an electron beam-cured hard paint film resulted in modulus reinforcement in the same manner as conventional thermosetting polymers. However, some behaviors were characteristic to the polymers in the present study. The degree of reinforcement was lower than the thermosetting polymers. The storage moduli of the composites containing TiO_2 with different surface treatments showed no significant difference, although thermosetting polymers showed greater reinforcement when the filler-polymer interaction was stronger.

Temperature dependence of the relative modulus and reduced damping were explained by the particle agglomeration theory. For the thermosetting polymers below the glass transition temperature, the relative modulus increases and the reduced damping decreases with increasing temperature, respectively. By contrast, the relative modulus showed no increase and the reduced damping showed no decrease by increasing temperature in the present polymers. This indicates that the present polymer is hard enough to exert large forces on the agglomerates to destroy them. It is also noted that stress

relaxation process around a particle will not be involved in increasing temperature, as the cross-linking was carried out at room temperature. Lower filler reinforcement compared with thermosetting polymers can be explained by the agglomerates destruction theory, and by reduced E_2/E_1 ratio. These explanations also can be adapted to the reinforcement difference between the PETA- and TMPTA-based polymers.

References

1. T. Shiota and M. Itoh, unpublished results.
2. M. Itoh, T. Shiota, and M. Nishihara, *Trans. Iron Steel Inst. Japan*, **25**(1), B-16 (1985).
3. H. M. Smallwood, *J. Appl. Phys.*, **15**, 758 (1944).
4. E. Guth, *J. Appl. Phys.*, **16**, 20 (1945).
5. E. H. Kerner, *Proc. Phys. Soc. London*, **69B**, 808 (1956).
6. Y. Sato and J. Furukawa, *Rubber Chem. Tech.*, **35**, 857 (1962).
7. Y. Sato and J. Furukawa, *Rubber Chem. Tech.*, **36**, 1081 (1963).
8. L. E. Nielsen, *J. Appl. Polym. Sci.*, **10**, 97 (1966).
9. L. E. Nielsen, *J. Composite Mater.*, **1**, 100 (1967).
10. K. Sato, *Prog. Org. Coat.*, **4**, 271 (1976).
11. S. Friedman, M. L. Kaufman, W. A. Steiner, and I. Wender, *Fuel*, **40**, 33 (1961).
12. W. T. Smith, *Off. Dig.*, **28**, 232 (1956).
13. M. Akay, S. J. Bryan, and E. F. T. White, *J. Oil Col. Chem. Assoc.*, **56**, 86 (1973).
14. T. Izumo and S. Yamamoto, *J. Japan Soc. Colour Material*, **55**, 804 (1982).
15. M. Tsubota, S. Furukawa, and K. Ueki, *J. Japan Soc. Colour Material*, **53**, 644 (1980).
16. M. Tsubota and K. Ueki, *J. Japan Soc. Colour Material*, **55**, 69 (1982).
17. M. Tsubota, A. Takahira, and K. Ueki, *Kobunshi Ronbunshu*, **35**, 87 (1978).
18. M. Tsubota and K. Ueki, *Kobunshi Ronbunshu*, **36**, 117 (1979).
19. W. Funke, *J. Oil Col. Chem. Assoc.*, **50**, 942 (1967).
20. B.-L. Lee and L. E. Nielsen, *J. Polym. Sci. Polym. Phys. Ed.*, **15**, 683 (1977).
21. K. Sato, *J. Japan Soc. Colour Material*, **37**, 473 (1964).
22. K. Sato, *J. Japan Soc. Colour Material*, **39**, 629 (1966).
23. K. D. Ziegel, *J. Colloid Interface Sci.*, **29**, 72 (1969).
24. K. D. Ziegel and A. Romanov, *J. Appl. Polym. Sci.*, **17**, 1119 (1973).
25. L. E. Nielsen, *Mechanical Properties of Polymers and Composites*, Marcel Dekker, New York, 1975.
26. L. E. Nielsen, *J. Polym. Sci. Polym. Phys. Ed.*, **17**, 1897 (1979).
27. L. E. Nielsen and T. B. Lewis, *J. Polym. Sci. A-2*, **7**, 1705 (1969).

Received June 12, 1987

Accepted August 24, 1987